Article

Risk Analysis and Visualization of Merchant and Fishing Vessels Collision In Coastal Waters

Chuanguang Zhu , Jinyu Lei , Zhiyuan Wang , Decai Zheng , Chengqiang Yu , Mingzhong Chen , Wei He [*]

Article

Risk Analysis and Visualization of Merchant and Fishing Vessels Collision in Coastal Waters

Chuanguang Zhu [1,2], Jinyu Lei [1,2,3], Zhiyuan Wang [1,2], Decai Zheng [4], Chengqiang Yu [2], Mingzhong Chen [4] and Wei He [1,2,*]

[1] School of Transportation, Fujian University of Technology, Fuzhou 350118, China
[2] Fujian Engineering Research Center of Safety Control for Ship Intelligent Navigation, College of Physics and Electronic Information Engineering, Minjiang University, Fuzhou 350108, China
[3] College of Computer and Data Science, Minjiang University, Fuzhou 350108, China
[4] Fuzhou Aids to Navigation Division of Eastern Navigation Services Center, Maritime Safety Administration, People's Republic of China, Fuzhou 350004, China
* Correspondence: hewei11@mju.edu.cn; Tel.: 0591-83761115

Abstract: The invasion of ship domain stands out as a significant factor contributing to the risk of collisions during vessel navigation. However, there is a lack of research on the mechanisms underlying collision risks specifically related to merchant and fishing vessels in coastal waters. This study proposes an assessment method for collision risks between merchant and fishing vessels in coastal waters and validated through a comparative analysis through visualization. First of all, the operational status of fishing vessels is identified. Collaboratively working fishing vessels are treated as a unified entity, expanding their ship domain during operation to assess collision risks. Secondly, to quantify the collision risk between ships, a collision risk index (CRI) is proposed and visualized based on the severity of collision risk. Finally, taking the high risk area of merchant and fishing vessels collision in the Minjiang River Estuary as an example, this paper conduct the analysis involves classifying ship collision scenarios, extracting risk data under different collision scenarios, and visually analyzing areas prone to danger. The results indicate that this method effectively evaluates the severity of collision risk, and the identified high-risk areas resulting from the analysis is verified by accidents occurred in the recent three years.

Keywords: merchant and fishing vessels collision; coastal waters; ship domain AIS; data visualization

1. Introduction

In recent years, the marine fishing industry has undergone rapid expansion, emerging as a pivotal facet within the maritime fisheries sector. The proliferation of fishing vessels has led to a discernible increase in channel congestion, making the navigational environment more intricate and increasing the potential of collision risks. Despite the integration of GPS, AIS, and the Beidou positioning system in many fishing vessels, merchant vessels often lack familiarity with the operational practices, methods, and working domains of fishing vessels. Consequently, insufficient attention is devoted to fishing zones and areas with a heightened risk of collisions. And effective communication between merchant and fishing vessels during hazardous situations proves challenging, culminating in collision incidents. Moreover, the visualization of high-risk navigational areas prone to collisions between merchant and fishing vessels holds paramount significance for maritime safety. Firstly, it can issue navigational hazard warnings to vessels in areas characterized by high navigational density, thereby mitigating the occurrence of maritime accidents. Secondly, with a comprehensive understanding of the primary navigation routes and operational domains of merchant fishing vessels, targeted supervision within these areas can be implemented by maritime authorities. However, devising a risk quantification model to assess collision risks between merchant and fishing vessels in different areas remains challenging due to the disparate maneuvering characteristics, navigational environments, and risk standards associated with these vessel types.

At present, the analysis of ship collision risk under different navigation conditions can be mainly divided into qualitative analysis and quantitative analysis. Regarding the qualitative analysis of vessel collision risks, Viktor [1] has introduced a fuzzy linguistic model to determine collision risk levels for vessels in busy traffic areas. This model comprises 22 terms within five fundamental term sets, each endowed with membership function parameters and a total of 200 fuzzy rules are generated to delineate collision risk levels. Additionally, Mira [2], leveraging fuzzy reasoning and Discrete Event System Specification (DEVS) theory, has proposed a novel model for predicting vessel collision risks while considering general collision avoidance patterns. This innovative model anticipates collision risks by forecasting changes in future vessel movements and validates the functionality of the model structure and fuzzy reasoning module through simulation experiments. In the domain of quantitative analysis for vessel collision risks, scholars often employ the concept of Closest Point of Approach (CPA) for situational analysis. Chin et al. [3] from the National University of Singapore have established a collision risk regression model for port waters based on CPA. In this model, Distance to Closest Point of Approach (DCPA) and Time to Closest Point of Approach (TCPA) is a pivotal factors determining collision risks.

In order to study the characteristics, causes and risks of collision accidents between merchant and fishing vessels, scholars have adopted various methods and models for analysis, and put forward corresponding conclusions or strategies, such as risk assessment analysis method [4,5] (Liu, K. et al., 2021; Yu, Y. et al., 2021), navigator collision avoidance behavior model and navigator error development process model [6], machine learning method [7], and probability risk assessment (PRA) models [8]. Mou et al. [9] constructed a linear regression model employing AIS data collected from collision avoidance scenarios in busy waterways. The study ascertained correlations between vessel size, speed, and heading with Distance to Closest Point of Approach (DCPA). Additionally, the researchers proposed a dynamic method for risk assessment based on Safety Assessment Model for Shipping and Offshore on the North Sea (SAMSON). Uğurlu et al. [10] compiled statistics on the causes of accidents involving fishing vessels during the period from 2008 to 2018. Based on the identified causes of fishing vessel accidents, the researchers constructed a Bayesian network to estimate the probabilities of accidents risk occurred under various circumstances.

In terms of mitigating the risk of collision between merchant and fishing vessels, many researchers have put forward related approaches from different perspectives. These include ship-to-ship dialogue and protocols [11], human-machine cooperative collision avoidance systems [12], requirements for fishing vessels [13], safe navigation for merchant vessels [14], and collision avoidance methods during fishing seasons [15]. Xu Xiaoming et al. [16] systematically summarized the patterns of collisions between merchant and fishing vessels, proposing preventive measures from aspects such as personnel, vessels, environment, and management. Chou et al. [17] conducted studies on collision accidents involving fishing vessels in different water regions. They delineated the risk and causes of collisions between fishing and non-fishing vessels, aiming to reduce incidents involving both types of vessels. In a study focused on preventing fishing vessel collisions, Seo et al. [18] developed a safety navigation system which can simultaneously receive the positions of smartphones and AIS information from vessels. It issues warnings to both merchant and fishing vessels when another vessel approaches within a 500-meter range. However, these studies specifically focused on collision prevention for fishing vessels have limitations, which is because fishing vessels exhibit significant heading deviations, making it challenging to achieve precise risk predictions solely based on distance, DCPA, and TCPA.

While there is a wealth of research on ship collisions, studies specifically focusing on collisions between merchant and fishing vessels in coastal waters are scarce. These studies often overlook the individual differences between merchant and fishing vessels at the time of collision, failing to consider the impact of fishing vessels in operational states on collisions. Therefore, this paper conducts a collision risk analysis of merchant and fishing vessels on vessel traffic data during the fishing season in the coastal areas of Fujian. Initially, the study initially adopts concepts from the ship domain and incorporates considerations for the operational status of fishing vessels to extract potential collision risk event from historical AIS data. Subsequently, a comprehensive visualization

analysis of the spatial distribution of encounters between merchant and fishing vessels is undertaken using the weighted kernel density estimation method. Finally, the paper identifies high-risk collision areas between merchant and fishing vessels based on the density of spatial distributions. The subsequent organization of the paper is as follows: Chapter 2 introduces the preprocessing of historical AIS trajectories and defines encounter risks based on ship domain and the operational status of fishing vessels. Chapter 3 systematically extracts encounter risk data between merchant and fishing vessels from historical records and conducts spatial and temporal analyses using the weighted kernel density method. Chapter 4 examines accident data from the past three years in the study area and conducted validations of the collision risk assessment algorithm proposed in this paper. Chapter 5 provides a summary and highlights the shortcomings of this paper.

2. Methodology

This paper utilizes historical AIS data from the coastal areas of Fujian to establish a ship collision risk model for the research and analysis of collision risks between merchant and fishing vessels. Firstly, the historical AIS data are processed and the encounter risk data are extracted on the basis of ship domain and the operational status identification of fishing vessels. Subsequently, a weighted kernel density estimation visualization method is employed to display encounter risk data, facilitating the identification of navigational areas prone to collision risks. Lastly, the approach is validated using the locations of ship collisions occurred within the research area over the past three years. The workflow of this paper, as illustrated in Figure 1, primarily comprises four modules: (1) AIS data preprocessing; (2) identification of fishing vessel operational states; (3) extraction of encounter risk data; and (4) visualization of encounter risk data.
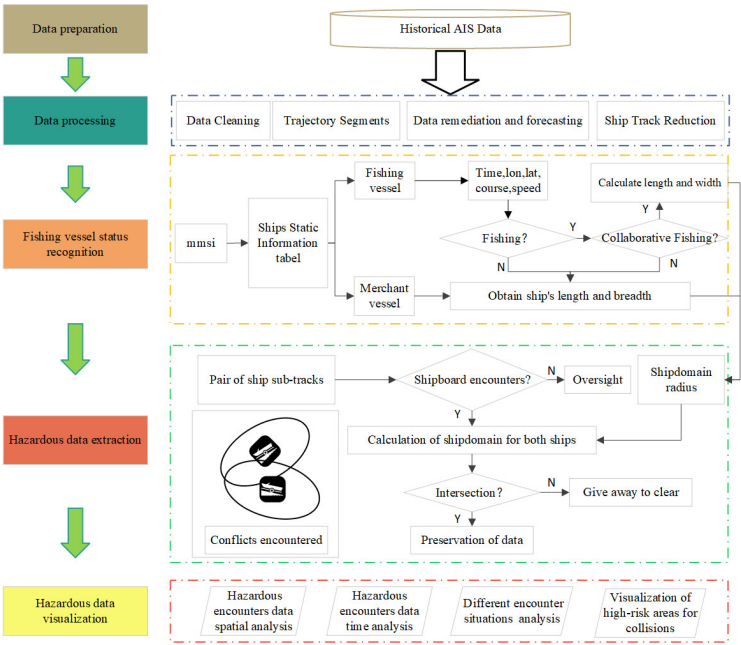

Figure 1. Visualization and assessment method for collision risks between merchant and fishing vessels in coastal waters.

2.1. Data Preprocessing

Due to issues such as location offsets and data losses in the raw AIS data, the analysis of collision risk areas between merchant and fishing vessels based on historical AIS data necessitates preprocessing of the raw data. Processing historical AIS data for merchant and fishing vessels includes data cleaning, trajectory separation, and the repair and prediction of AIS data. Finally, vessel static infomation are queried based on MMSI to distinguish between merchant and fishing vessels, providing an analytical foundation for assessing collision risks between these two types of vessels.

2.1.1. Data cleaning

The data cleaning process primarily involves removing abnormal and duplicate data from AIS data. Abnormal data includes the following situations:

(1) Geographical coordinates located on land;
(2) Values exceeding the normal range (refer to Table 1 for data range);
(3) MMSI not conforming to specifications.

Table 1. Data range of the study area.

Parameters	Type	Range
Time	timestamp	2022/08/01–2022/12/01
MMSI	text	200000000 - 799999999
Longitude	float	0-180°
Latitude	float	0-90°
SOG	float	0-20kn
COG	float	0-360°
Heading	float	0-360°

The occurrence of duplicate data is primarily attributed to the repetitive transmission of AIS data by anchored vessels. As the experiment primarily focuses on the potential risks associated with moving vessels, it is necessary to eliminate AIS data for vessels at anchor.

2.1.2. Trajectory Separation

When analyzing collision risks between merchant and fishing vessels, it is crucial to identify different behavior patterns of vessels accurately by considering key features such as location, time, heading, and speed. In order to reconstruct the historical navigation behavior of vessels, trajectory separation is necessary. Trajectory separation involves two main tasks: one is to separate the trajectory data of different ships according to MMSI; Second, separate different trajectories from the same ship. Firstly, according to the data characteristics of AIS data, MMSI is the unique identification between different ships and can be used as the basis for separating different ship trajectories. Here, we directly group AIS data according to MMSI to obtain trajectory data of different ships. Secondly, different trajectories of the same ship are separated according to the AIS data receiving time interval and the distance between adjacent points. The algorithm process of trajectory segmentation is shown in Figure 2:
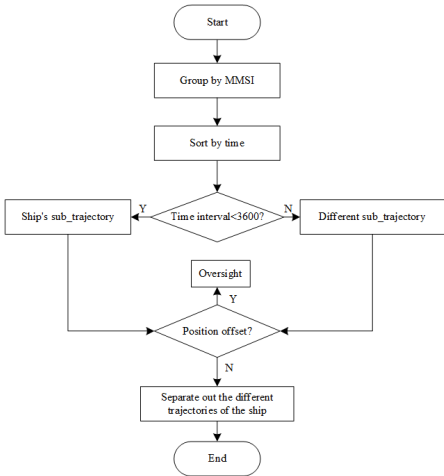

Figure 2. Schematic diagram of trajectory segmentation algorithm.

The experiment selects 1 hour as the time interval to determine whether the trajectories before and after the interval are consistent. In addition, the distance between adjacent two points is also used as the basis for judgment. According to the calculation of the ship speed of 0-20knot, the sailing distance every three minutes is within 0-1 nautical miles. If the distance is excessively large, it is deemed to indicate equipment failure or latitude and longitude drift, leading to the direct exclusion of such points. The latitude and longitude in AIS data adopts WGS84 coordinate system, and the distance of any two points can be calculated by formula (1) - (3) :

$$C = \sin{(y_{i-1})}\sin{(y_i)} + \cos{(y_{i-1})}\cos{(y_i)}\cos{(x_{i-1} - x_i)} \quad \text{i=2,3,...,m-1,m} \quad (1)$$

$$D = R^*\arccos{(C)}^*(\frac{\pi}{180}) \quad (2)$$

$$v_m = v_k * 0.518 \quad (3)$$

In the processing, the separated AIS trajectory points are grouped into sub-trajectories and connected based on time in ascending order. This process further reconstructs the historical navigation path of the vessels, as shown in Figure 3. The processed data clearly reveals the main channels of vessel navigation and points of trajectory intersection.
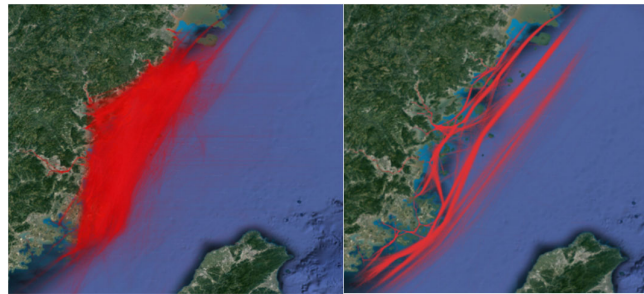

Figure 3. Comparison of effects before and after data pretreatment (a. before preprocessing; b. after preprocessing).

2.1.3. Data Restoration

In the actual data collection process, AIS data reception can be affected by sensor noise and external environmental factors, leading to issues such as data loss. To ensure the temporal synchronization and high-frequency of AIS data for various vessels, interpolation and resampling of AIS data are necessary to conduct. Based on the proposals in references [19,20], which suggest that, in the absence of prior experience, using Piecewise Cubic Hermite (PCH) interpolation yields minimal errors in reconstructing missing data. Therefore PCH interpolation method is applied in this study to restore AIS data.

2.2. *Identification of Fishing Vessel Operation Status*

The status of the fishing vessels is crucial to define the avoidance distance of passing ships, and the operating status of the fishing vessel should be taken into account when judging the risk of collision. In this experiment, the analysis of AIS trajectory data in the research area during fishing operations reveals distinctive features. Different rules are established to identify the operational states of fishing vessels, and varying safety encounter distance thresholds are set based on the specific state of each fishing vessel.

2.2.1. Characteristics of Fishing Vessel Operational Trajectories

Different fishing methods exhibit distinct trajectory characteristics during fishing operations. Fishing vessel operations can be classified into three main categories, which mainly includes trawling operation, purse seine operation and gillnet operation. Trawling operation is the trawling of fishing gear along the seabed to catch fish. Purse seining entails surrounding a school of fish with a net to

capture them; Gillnet operation employs a long net suspended vertically in the water to entangle fish. The trajectory characteristics for each of these fishing methods are as follows:
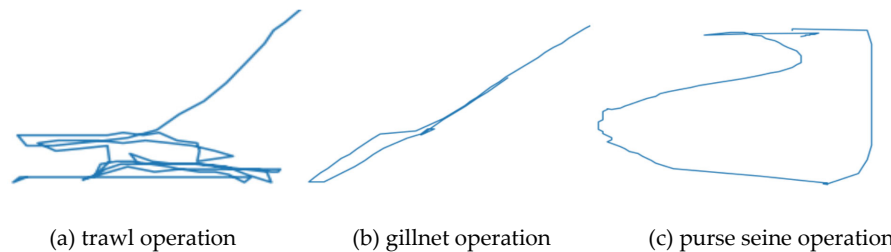

(a) trawl operation   (b) gillnet operation   (c) purse seine operation

Figure 4. Characteristics of fishing vessel operational trajectories under different operating modes

The typical trajectory characteristics for different fishing operation are as follows:
- Trawl operation: Characterized by frequent turns during operations, towing the net back and forth in a specific area.
- Gillnet operation: Marked by dropping numerous drifting gillnets along a trajectory and returning along the same path to retrieve the nets.
- Purse seine operation: Distinguished by deploying the net to encircle a target area, returning to the starting point, and then retrieving the net.

2.2.2. Fishing Boat Operation Status Judgment

In the study, the operational states of fishing vessels are categorizes into three modes: normal navigation, anchorage, and active fishing. The criteria for each state are defined as follows:
1. Normal Navigation: Fishing vessels engaged in normal navigation exhibit relatively stable speed and direction, with no abrupt changes. Vessels with speeds greater than 2 knots and maintaining stable speed and heading within a 10-minute interval are identified as in a normal navigation state.
2. Anchorage: Vessels at anchor may exhibit some speed due to factors like sea currents. Therefore, In the processing, vessels with speeds below 2 knots and a substantial number of AIS data positions in close proximity, exhibiting a movement distance less than 0.1 nautical miles within a 10-minute interval, are identified as vessels at anchor.
3. Fishing: Identifying whether a fishing vessel is actively fishing relies on distinguishing trajectory characteristics that differ from normal navigation. Fishing vessels typically operate at speeds ranging from 2 to 5 knots. we identifies vessels within this speed range and examines their trajectories to determine if they are engaged in fishing. If nearby vessels are also in a fishing state and within 0.5 nautical miles, it is considered as cooperative fishing. During this operation, the fishing vessel's maneuverability is limited, and passing merchant vessels are advised to maintain a distance of at least 1 nautical mile.

2.3. Encounter Risk Data Mining and Visualization

Establishing an effective model for identifying vessel navigation risks is crucial for extracting encountering risk data. This paper constructs a model for identifying vessel encounter risks based on ship domain. Then, this model is employed to extract data relate to vessels encountering risks, and further quantifies collision risk by calculating the CRI. Firstly, the DCPA and TCPA are computed for pairs of vessels that may encounter each other. It is considered that vessels with DCPA less than 2 nautical miles and TCPA less than 20 minutes may pose encounter risks. The encounter risk is further determined by calculating whether there is an intersection in the vessel domains. Finally, the data related to encounter risks is saved, and visualization tools such as QGIS and Folium are employed for the analysis of encounter risk data.

2.3.1. Ship Domain Model

In the early 1960s, Japanese scholar Fujii [21] et al. proposed the concept of ship domain when studying the traffic capacity in the waters near Japan, and tried to establish the calculation method of ship domain when ships navigated in narrow waters. According to this model, the ship domain is an elliptical area centered around the vessel, with the major axis aligned with the vessel's heading and the minor axis perpendicular to the vessel's heading. The variables a and b represent the major and minor axes, determining the elliptical domain with the condition 0 < a < b. As illustrated in Figure 5, specific values for a and b can be chosen based on the actual circumstances.

Figure 5. Fujii ship domain model.

This paper employs the Fujii model to determine the values of the major axis (a) and the minor axis (b) for the elliptical ship domain of vessels during normal navigation, as expressed in Equation (4). Here, l represents the vessel's length, and w represents its width.

$$\begin{cases} a = 1.5 \times l \\ b = 1.5 \times w \end{cases} \tag{4}$$

In the case of fishing vessels engaged in operations, occurrences such as obstructive fishing nets render the classical elliptical ship domain inapplicable. Since the length of a single trawl net should be limited to within 600 meters for navigational safety, passing merchant ships are required to maintain a distance greater than 0.5 nautical miles. Therefore, for fishing vessels operating individually, the ship domain radius is set to 0.5 nautical miles, as depicted in Figure 6(a). Furthermore, for fishing vessels engaged in coordinated operations, they are treated as points on a polygon. The circumscribed circle of the polygon is considered as a whole when calculating the ship domain, ensuring that the encounter distance for each fishing vessel is not less than 0.5 nautical miles, as shown in Figure 6(b).

(a) single-vessel operation   (b) multi-vessel collaborative operation

Figure 6. Schematic diagram of fishing vessel domain in operation.

2.3.2. Calculation of DCPA and TCPA

DCPA and TCPA are crucial parameters in determining the risk of ship collisions when vessels encounter. During calculation, one of the vessels is chosen as the reference vessel, establishing a coordinate system as illustrated in Figure 7.
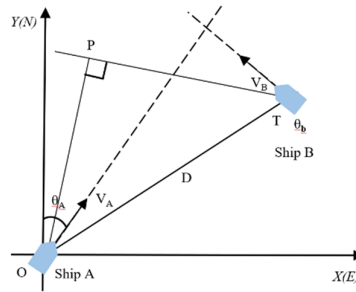

Figure 7. Schematic diagram of the encounter of two ships.

Assume that A is the own ship, lon_A、lat_A、V_A and θ_A are the longitude and latitude, speed and course of ship A respectively. B is the target ship, lon_B、lat_B、V_B and θ_B are respectively the longitude and latitude, speed and course of ship B, then the relative speed of the two ships is shown in formula (5) :

$$V_r = \sqrt{V_A^2 + V_B^2 - 2 \mid V_A \cdot V_B \mid \cos(\theta_B \cdot \theta_A)} \qquad (5)$$

DCPA and TCPA can be calculated by formula (6) - (8) :

$$DCPA = D \times \sin(\angle OTP) \qquad (6)$$

$$\mid TP \mid = \sqrt{\mid OT \mid^2 - \mid OP \mid^2} \qquad (7)$$

$$TCPA = \frac{\mid TP \mid}{V_r} = D \times \frac{\cos(\angle OTP)}{V_r} \qquad (8)$$

where D represents the relative distance between two trajectory points, which can be obtained from formula (2). Then, DCPA and TCPA are utilized for assessment of collision risks during vessel navigation and visualization of risk data.

2.3.3. Collision Risk Index

According to the definition of ship domains, encountering danger is considered when the domain of a navigating vessel is breached. However, it cannot be used to measure the magnitude of collision risk. In order to further quantify the risk after the invasion of the ship domain during the encounter, the CRI is introduced to quantify the collision risk. This paper evaluates the magnitude of collision risk throughout the entire ship encounter process by considering both the intersection of ship domains and collision risk index.

Among the calculation methods of CRI, Kearon[22] comprehensively considered the influence of DCPA and TCPA, and take into account both factors by using a weighted combination of DCPA and TCPA to determine CRI, as shown in Equation (9). However, its defect is that it does not consider the different dimensions of DCPA and TCPA, which has a certain impact on the results of CRI.

$$\rho_i = (a \cdot DCPA_i)^2 + (b \cdot TCPA_i)^2 (i = 1,2,\cdots,n) \qquad (9)$$

In order to reflect the different importance of DCPA and TCPA in the results of CRI, Weng Jianjun [23] conducted experiments, combined with typical collision cases, and considered the effects of the International Regulations for Preventing Collisions at Sea (COLREGs). They summarized a relationship Equation (10) for the importance of DCPA and TCPA in collision outcomes and provided different values for m (1.4, 1.3, 1.2, 1.1) under various situations.

$$DCPA_P = m \cdot TCPA_P \qquad (10)$$

The value of m depends on the different encounter orientation, and the specific value is as follows:
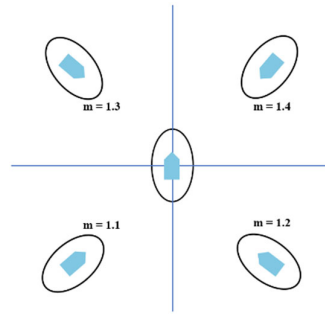

Figure 8. Schematic diagram of m values under different encounter orientation.

By combining equation (9) and (10), the method to determine the CRI in this paper is obtained, as expressed in equation (14). In the study, a = b = 1 is used for calculation.

$$\rho = (DCPA)^2 + (\frac{TCPA}{m})^2 \qquad (14)$$

2.3.4. Risk Data Extracting

Based on the ship domain theory, navigational encounter risk can be defined as a situation where two or more vessels come into contact or overlap when encountering each other. The COLREGs defined three encounter situations: head-on, crossing, and overtaking. However, COLREGs only quantitatively defined overtaking situations and did not provide quantitative definitions for crossing encounters and head-on encounters. To extract risk data in different encounter scenarios, the experiment divides ship encounter situations based on the difference in heading between two ships, as illustrated in Figure 9.
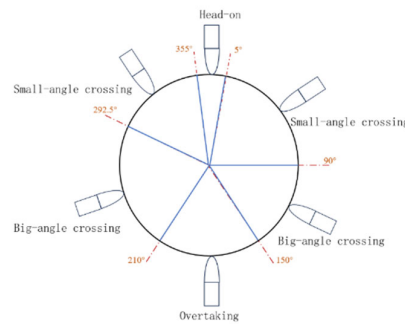

Figure 9. Classification of encounter situations.

The process of extracting encounter risk data involves three primary steps. Firstly, it is essential to determine whether an encounter situation has arisen between the own ship and the approaching vessel. According to the COLREGs, the masthead light visibility distance is specified as 6 nautical miles for vessels with a length exceeding 50 meters. Therefore, we only compute the DCPA and TCPA for vessels within a 6 nautical mile radius of the own ship. It is considered that an encounter situation exists with the closest vessels' DCPA less than 2 nautical miles. Secondly, further calculations are performed to determine whether there is an overlap in the ship domains. If ship domains intersect, the encounter data is stored in different encounter scenario datasets based on their relative positions during the encounter. Finally, computation of CRI for the vessels involved in the encounter is performed. The algorithm flow is illustrated in the diagram below:
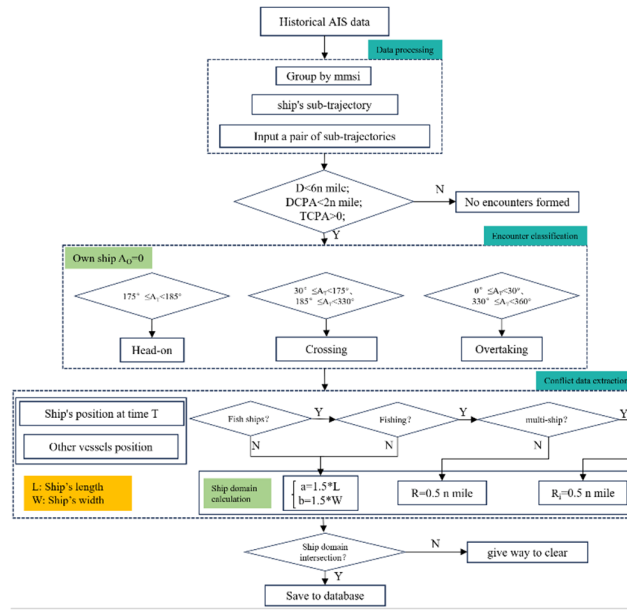
10

Figure 10. Schematic diagram of dangerous encounter extraction algorithm.

2.3.5. Risk Data Visualization

Risk data visualization enables the concise and intuitive display of spatial distribution patterns, revealing deeper insights. QGIS (Quantum GIS) is a user-friendly open-source desktop GIS software with powerful analysis capabilities, making it suitable for conducting visual analysis on vessels' encounter risk data. Figure 11 is based on the historical AIS track data of the coastal area of Lianjiang County, Fujian Province, combined with the navigation environment of the coastal area of Fujian Province and the status quo of customary shipping routes, traffic flow rules, conflict risk of merchant fishing vessels, and ship track clustering analysis to obtain the visualization effect of merchant and fishing vessels. Figure 11 illustrates the visualization of vessels' trajectories using QGIS software. This visualization is based on historical AIS trajectory data along the coastal waters, combined with the navigational environment and the analysis of traffic flow.
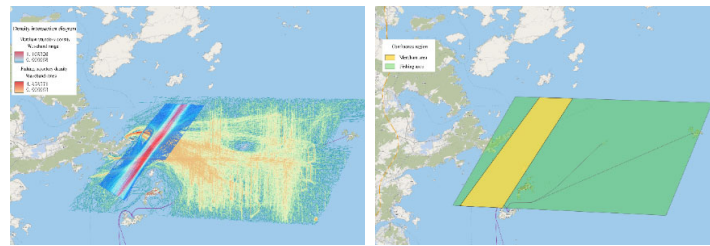

Figure 11. Overlapping channels of merchant and fishing vessels.

Kernel density analysis of ship trajectory data can also be performed using QGIS, which can display different colors by calculating the density in each raster pixel, and can more intuitively show the navigational density situation and risk severity in different encounter situations. As shown in Figure 12 is the effect of kernel density visualization of the original trajectory data in the coastal waters. Moreover, in the visualization of the risk level during encounters, different weights can be used to visualize the encounters risk data in different areas according to the CRI.
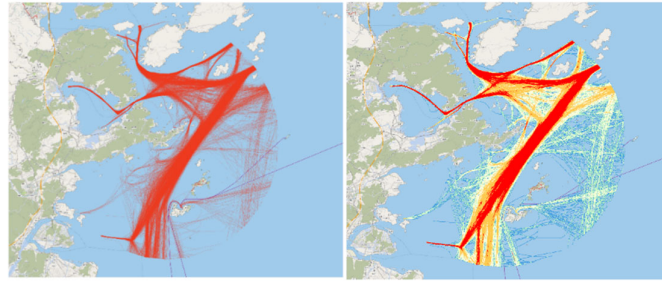
Figure 12. Comparison of raw and weighted kernel density trajectory visualizations.

3. Experiments

The fishing season is a peak period for collisions involving commercial and fishing vessels. Therefore, the experiment focuses on AIS data from the coastal areas of Fuzhou during the autumn fishing season from August, 2022, to November, 2022. The study aims to extract data related to hazardous encounter scenarios and analyze high-risk areas and peak periods for collisions between commercial and fishing vessels along the Fuzhou. Given the limited consideration of fishing vessel operational status in past analyses of collision risks between commercial and fishing vessels, this study analyzes collision risks during vessel encounters based on the ship domain theory and takes into account factors such as the fishing vessel's operational status, encounter situations between vessels, vessel types, relative speeds, and day-night environmental conditions. The study involves separating trajectories of commercial and fishing vessels from massive AIS data, identifying the fishing vessel's operational status, and extracting information related to hazardous vessel encounters. It further analyzes the spatial distribution of risky encounter data and examines distribution characteristics related to vessel types, vessel dimensions, and vessel speeds involved in hazardous encounter scenarios. Additionally, the study analyzes the temporal distribution of hazardous encounter data, exploring distribution characteristics over time.

3.1. Analysis of the Characteristics of Dangerous Vessels

3.1.1. Ship Type Distribution in Encounter Scenarios

The experiment statistically analyzed the histogram of the distribution of ship length and width involved in dangerous encounters. The histogram revealed that the lengths of fishing vessels involved in dangerous encounters were   predominantly concentrated in the range of 30-50m, with widths between 5-10m. On the other hand, merchant ships involved in dangerous encounters showed a concentration of lengths between 50-150m and widths between 8-20m for small to medium-sized merchant ships. Typically, these smaller and medium-sized cargo vessels lack advanced equipment, making it challenging to promptly detect the position information of small fishing vessels, leading to a higher risk of collision. Additionally, the experiment conducted a statistical analysis of the distribution of ship types involved in dangerous encounters, as illustrated in Figure 13. Out of the 6442 vessels involved in dangerous encounters, fishing vessels accounted for the largest proportion at approximately 61.8%, followed by merchant vessels at around 28.86%. This highlights that cargo and fishing vessels are the primary types contributing to maritime accidents in this area.
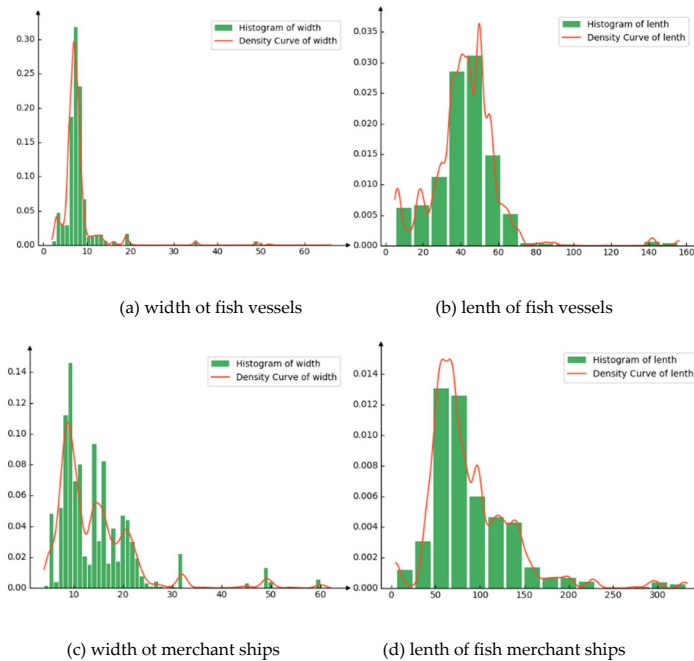
(a) width ot fish vessels (b) lenth of fish vessels

(c) width ot merchant ships (d) lenth of fish merchant ships

Figure 13. Histogram of frequency distribution of ship length and width.
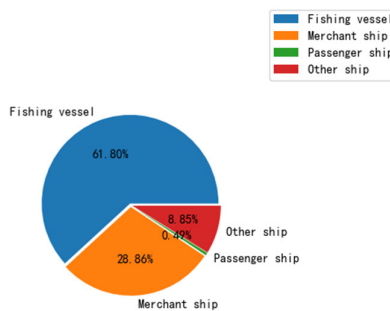

Figure 14. Distribution of vessel types involved in hazardous encounters.

Encounter Situations speed Distribution

A statistical analysis of vessel speeds is presented in different encounter situations shown in Figure 15. Overall, there is a similar trend in the distribution of speeds, with a higher proportion falling within the 7-10 knots range. Specifically, for vessels involved in head-on encounters, their speed distribution follows a Weibull distribution, as depicted in Figure 15(a). The majority of speeds are in the 8-10 knots range, accounting for 50.47\%, with an average speed of approximately 8.23 knots. In the case of vessels involved in crossing encounters, their speed distribution follows a distribution as shown in Figure 15(b). The predominant speeds are in the 8-10 knots range, constituting 39.7\%, with an average speed of 7.5 knots. For vessels involved in overtaking encounters, their speed distribution is illustrated in Figure 15(c). The majority of speeds are between 8-10 knots, making up 46.1\%, with an average relative speed of approximately 7.94 knots. Notably, vessels involved in overtaking and crossing encounters exhibit lower average speeds compared to vessels in head-on encounters in hazardous encounter scenarios.
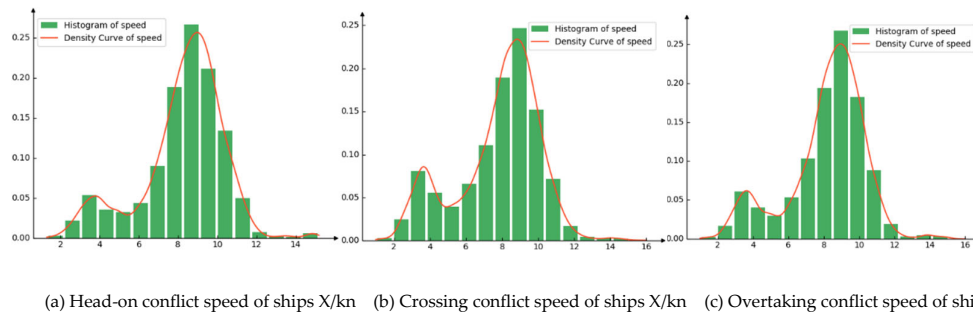
(a) Head-on conflict speed of ships X/kn   (b) Crossing conflict speed of ships X/kn   (c) Overtaking conflict speed of ships X/kn

Figure 15. Histogram of collision velocity distribution of different collision situations.

A heat map illustrating the velocity distribution of hazardous vessels within the study waters is depicted in Figure 16. It can be seen from the figure that the ship speed in the hazardous encounter scenario from the internal route to the external route along the coast of Fuzhou presents an increasing distribution. The speed of the external route is significantly higher than that of the internal route, which is closely related to the wide sea depth and fewer obstacles on the external route.

Figure 16. Heat map of speed distribution in danger.

3.2. Spatial Distribution of Hazardous Encounter Events

Based on the spatial distribution of ship hazard encounter events depicted in Figure 17, hazardous encounters along the Fujian coast are predominantly concentrated in four regions. These regions are the entrances of bays (such as Sansha Bay) or Minjiang River, and the fishing port areas (such as Tailu Fish Port). A conflict peak is observed in the entrance waters of Sansha Bay, forming due to the fact that this is the sole entrance and exit of Sansha Bay. During the fishing season, numerous fishing vessels navigate through this area, and the complex navigation conditions, including obstacles such as reef islands in the middle of the channel, contribute to the dense distribution of collision conflicts. The secondary conflict values are located from Guanbei Island to the main channel of the Minjiang River estuary. This area is a mandatory passage for fishermen from Tailu Town entering and leaving the fishing port, intersecting with the traffic flow to and from the Minjiang River Estuary. With a higher navigation density, the likelihood of maritime collision accidents is significantly increased.
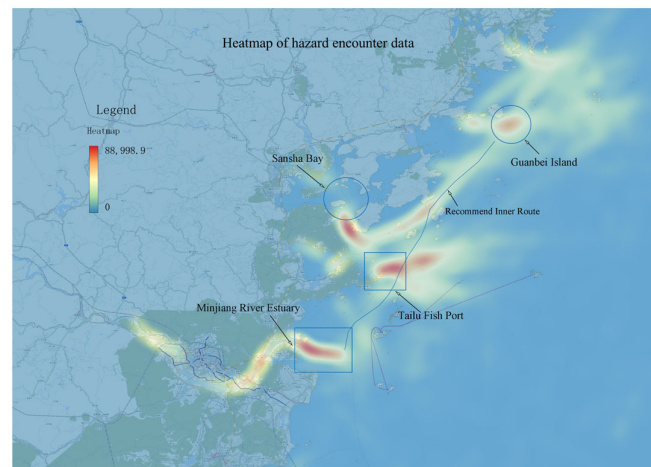
Figure 17. Spatial distribution of risk encounter data.

3.2.1. Spatial Distribution of Head-on Encounter Hazardous Scenarios

The most intensive area of head-on hazardous events situated near the entrance of Sansha Bay as illustrated in Figure 18. This area serves as the exclusive entry and exit point for fishermen heading out to sea in Sansha Bay. The presence of navigational constraints such as reefs on the southern side creates a traffic bottleneck, making it a high-traffic area prone to head-on encounter conflicts between commercial and fishing vessels. The conflicts are particularly pronounced within the primary shipping lane, emphasizing the prevalence of head-on encounter issues in this region. The second-highest density of head-on encounter hazardous events is observed in the nearshore waters. This area functions as a major transportation hub for fishermen from Tailu Town and intersects with the recommended inland waterway connecting Guanbei Island and the Min River Estuary. The notable conflict arises from encounters between southbound and northbound commercial vessels and fishermen heading out for fishing activities. The conflicts are widespread in this area due to the high volume of fishing vessels.
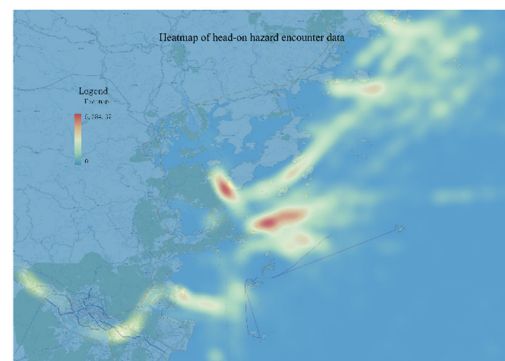

Figure 18. Spatial Distribution of Head-on Encounter Hazardous Scenarios.

Spatial Distribution of Crossing Encounter Hazard Scenarios

Crossing encounter hazard events constitute the predominant type of maritime conflicts in the research area, accounting for a substantial 63.14%. This highlights the significance of crossing encounter hazards as a primary concern for vessels navigating the strait. Figure 19 illustrates the spatial distribution of crossing encounter hazard events in the research area. The maximum concentration of crossing encounter hazards is located near the waters of the Minjiang River estuary. This area serves as a convergence point for river vessels from the Minjiang River and ocean-going commercial vessels entering the Minjiang River estuary. It is a crucial turning point for vessels

navigating from Guanbei Island to the main channel leading to the Minjiang River, creating a region with a broad distribution and high density of crossing encounter hazards. The second dense area of crossing encounter hazards is situated in the Sansha Bay. Vessels navigating through this area tend to make significant turns near Jigongshan, leading to crossing encounter situations. Limited visibility and the necessity for vessels to make substantial maneuvers increase the potential for dangerous encounters with passing vessels, posing a significant risk of collision.

Figure 19. Spatial Distribution of Crossing Encounter Hazard Scenarios.

Spatial Distribution of Overtaking Dangerous Scenarios

The spatial distribution of overtaking encounter hazard events within the studied area is illustrated in Figure 20. The primary hotspot for overtaking encounter hazard events is situated at the entrance and exit points of Sansha Bay and Luoyuan Bay, especially in the vicinity of Jigongshan when navigating the channel to and from Sansha Bay. The deceleration and acceleration of vessels during course changes in this area are likely the primary contributing factors to the occurrence of overtaking encounter hazard events. The second dense area of overtaking collision hazard events is in the region connecting Tailu Town and Haidao Town. This area is serving as a crucial intersection for fishermen from Tailu Town heading north to the open sea, utilizing the recommended waterway, and also serves as a convergence area for fishermen changing course to return to port. The likelihood of vessels accelerating and decelerating in this waterway is significant, making it a key factor in the numerous overtaking encounter hazard events observed in this area.
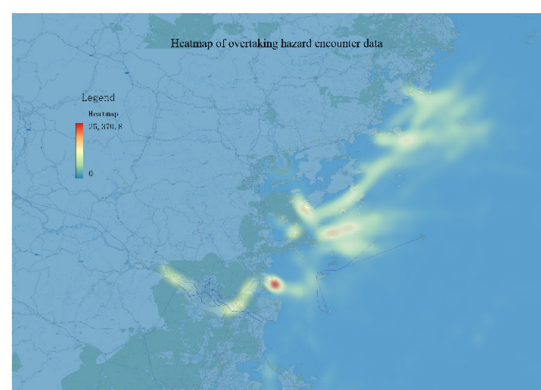

Figure 20. Spatial Distribution of overtaking dangerous Scenarios.

3.3. Temporal Distribution of Hazardous Encounter Data

The study area's fishing season is divided into two distinct periods: spring and autumn. The spring season spans from March to May, while the autumn season extends from August to November. The data utilized cover the period from August to November, corresponding to the autumn fish flood season. Fishing vessels typically navigate without a fixed course during the

operational process, involving both departure and return. These movements are generally determined by the tide and the abundance of fish. Typically, fishing vessels are small, limiting the use of large nets for deep-sea fishing. Consequently, they engage in small-scale fishing in the shallow waters near the sea. Due to the abundance of predators in shallow waters during the day, fish in these areas disperse, hide, or migrate to the deep sea. Consequently, fishermen opt to fish at night. To analyze the Temporal distribution of dangerous events involving fishing vessels, statistical analysis was applied to the AIS data of the study waters.

3.3.1. Distribution of Fishing Vessels in Hazard

The temporal distribution of encounter hazard events, as shown in Figure 21, reveals that a notable concentration during the evening hours from 6:00 PM to 12:00 AM. This period often considered the peak period for fishing activities. Navigational conditions become more complex during this time due to the onset of darkness, coupled with the fact that certain fish species exhibit increased activity during the night. Additionally, nighttime weather conditions at sea are typically more intricate than those during the day. The reduced visibility for crew members, coupled with fatigue from continuous work, significantly impacts their vigilance and responsiveness, thereby elevating the risk of maritime accidents.
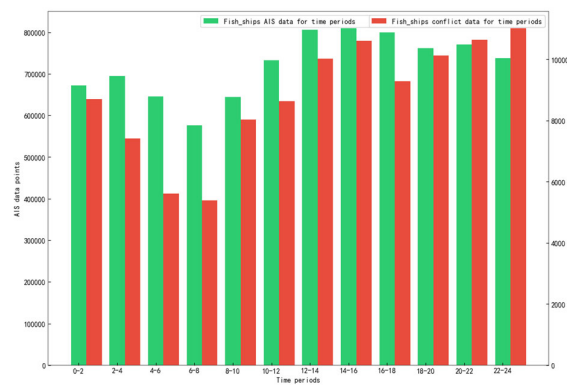

Figure 21. Temporal distribution of encounter hazard events.

3.3.2. Temporal Distribution of Hazardous Encounter Events under Different Scenarios

The temporal distribution of hazardous encounter events under various encounter scenarios is illustrated in Figure 22. Across all encounter scenarios, the primary timeframes for encountering risks are from 8:00 AM to midnight, with the least data recorded between 4:00 AM and 6:00 AM. However, the peak periods for encounter hazard events slightly differ among the encounter situations. For head-on encounters, the peak time occurs between 2:00 PM and 4:00 PM, while for crossing encounters, it is between 10:00 PM and midnight, and for overtaking encounters, it is between 12:00 PM and 4:00 PM.
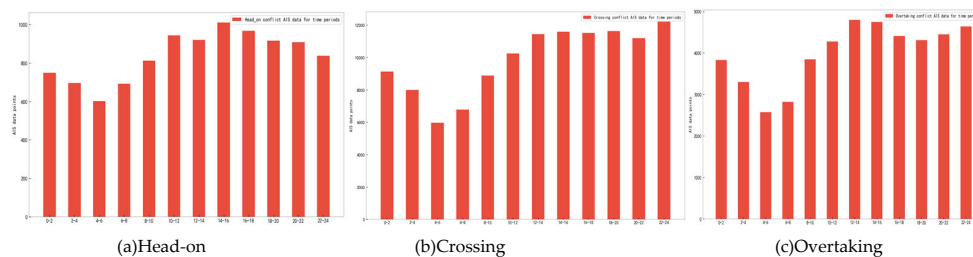

| (a)Head-on | (b)Crossing | (c)Overtaking |

Figure 22. Temporal distribution of hazardous encounter events under different scenarios.

3.3.3. Spatial and Temporal Distribution of Encounter Hazardous Events

The experiment incorporated the time dimension into the heat map. Figure 23 illustrates the thermal maps representing hazardous data during six time intervals: 0-4, 4-8, 8-12, 12-16, 16-20, and 20-24. The figure reveals a similar spatial distribution of hazardous encounter events across different time periods, with relatively dense concentrations along the east coast of the Lianjiang River, Shacheng Port, Sansha Port, and the Minjiang estuary. It exhibits a higher density during the period from 12 to 24, corresponding to the busy hours for fishermen. Typically, merchant ships and fishing boats navigate during this period, resulting in the intersection of their sailing paths, elevating the risk of ship encounters and potential collisions.
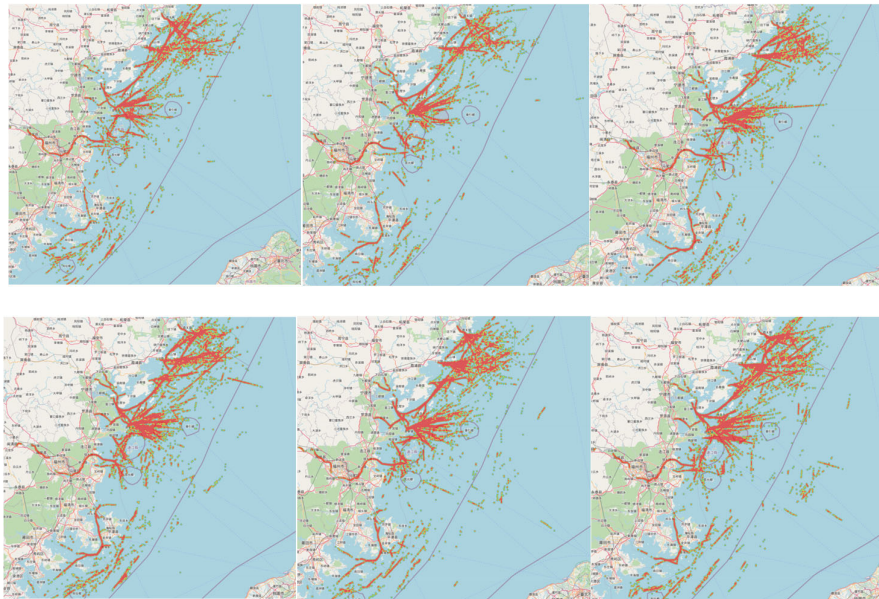

Figure 23. Heatmaps of encounter hazardous data in different time periods.

4. Analysis and Discussion

4.1. Case Analysis of Collisionaccidents

To validate the accuracy of the high-risk collision zones identified based on historical AIS data, this study gathered maritime accident data from the study area over the past three years. The analysis of accident occurrence regions was coupled with an examination of the causes behind these incidents. Furthermore, a comparison was made between the locations of six maritime collision incidents that occurred in the study area over the last three years and the high-risk collision zones identified above.

4.1.1. Marine Accident Data Statistics

According to data compiled by the Fuzhou Maritime Safety Administration, the total number of maritime incidents in the Fuzhou coastal waters from 2020 to 2023 was 33. Among these incidents, sinking accidents were the most prevalent, constituting 27.27% of the total, followed by collision accidents at 21.21%. Incidents involving shipwreck had the lowest proportion, accounting for a mere 3.03%. Major accidents in the coastal waters made up 12.12% of the total incidents, as depicted in Figure 24. General accidents accounted for 27.27%, while minor incidents were the most frequent, representing 60.61%.
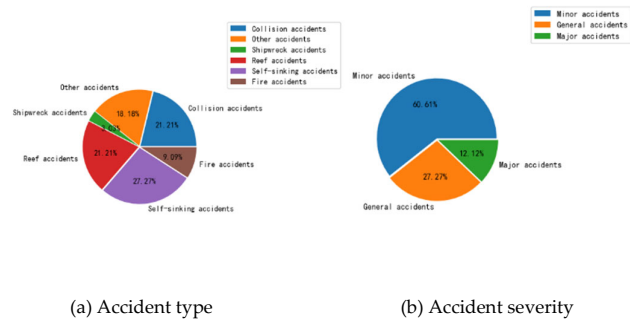
(a) Accident type   (b) Accident severity

Figure 24. Statistical diagram of ship accident data.

4.1.2. Analysis of High Risk Areas of Collision between Merchant Ships and Fishing Vessels

Merchant ships and fishing boats serve distinct purposes, resulting in varied sailing areas. To delve deeper into the analysis of collision high-risk areas for these vessels, the experiment presents heatmaps depicting the frequency of encounter risks for both types. The identified high-risk areas for merchant and fishing vessels are illustrated in Figure 25.

In the case of fishing vessels, the predominant incident-prone region is around the line connecting Tailu Town and Yangyu Island. This is attributed to the high volume of fishing vessels navigating through this area, overlapping with the recommended inner shipping route for merchant vessels. The complex interweaving of trajectories, narrow channels, numerous obstacles, and intricate water currents contribute to frequent accidents. Particularly, small to medium-sized wooden fishing vessels, with poor radar reflection and limited visibility, are prone to accidents in this region, as passing merchant vessels may struggle to detect their radar echoes effectively.

For merchant vessels, the primary incident-prone area is the exit of the Minjiang River channel. This region is characterized by numerous bends, and many merchant vessels tend to overlook radar blind spots, failing to exercise sufficient caution. There is a tendency to excessively rely on radar functionality, neglecting proper lookout procedures. Lack of essential experience and knowledge on utilizing radar echoes to detect smaller fishing vessels contributes to collisions in this area.
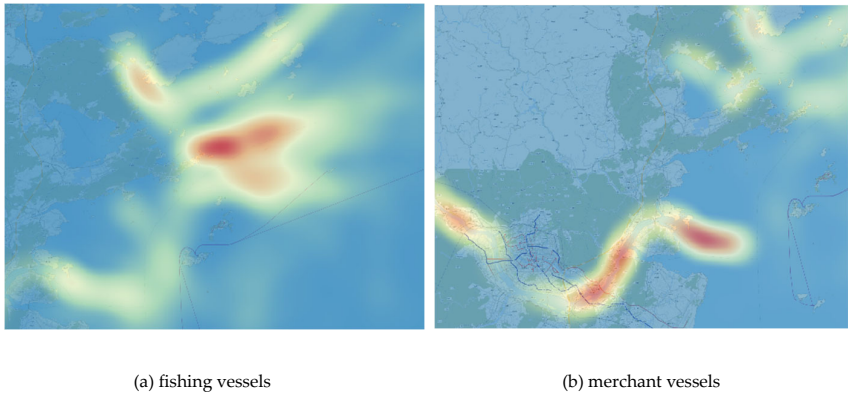

(a) fishing vessels   (b) merchant vessels

Figure 25. Heatmaps of high-risk areas for merchant and fishing vessels.

4.1.3. Comparison with Actual Collision Incidents

The analysis conducted in this study focuses exclusively on collision incidents. Therefore, a comparative analysis is performed between the areas where six collision incidents occurred in the past three years and the high-risk collision areas identified in this study. Figure 26 illustrates the comparison between the experimentally derived high-risk collision areas for merchant and fishing vessels and the actual regions where ship collisions occurred. Moreover, five out of the six collision incidents align with the areas identified as high-risk collision zones in this experiment. This

correspondence validates the effectiveness of the experiment's methodology in identifying high-risk collision areas for merchant and fishing vessels.
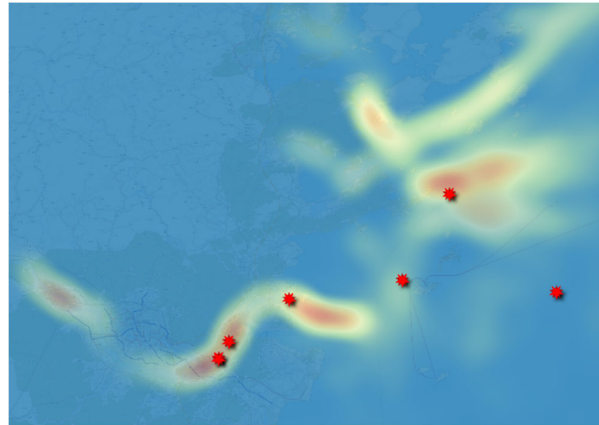

Figure 26. Comparison of merchant fishing vessel collisions and collision high hazard areas.

5. Conclusions

Based on the analysis of historical AIS data collected during the 2022 autumn fishing season in the study waters, this paper aims to identify areas prone to collision accidents involving merchant and fishing vessels with consideration of operating status of the fishing vessel. The aim is to identify areas prone to collisions between merchant and fishing vessels, providing a warning for vessels to exercise sufficient caution when navigating through high-risk zones and reduce the occurrence of maritime collisions. The experimental approach involves preprocessing historical AIS data to reconstructing the vessels trajectories. Subsequently, concepts such as vessel domain and collision risk index are employed to define hazardous encounter events, considering the operational states of fishing vessels to accurately depict real encounter situations. By assessing the frequency of hazardous encounter events, the study identifies high-risk collision areas. The primary research findings are summarized below:

1. Identification of Fishing Vessel Operational Status: The paper proposes a method to identify the operational status of fishing vessels. Recognizing the operational status of fishing vessels is crucial for collision prevention, particularly when encountering fishing vessels engaged in operations. The experiment distinguishes between the navigation trajectories of fishing vessels under different operational characteristics to effectively identify the operational status of fishing vessels, with a focus on those engaged in operations during encounter risk analysis.

2. Evaluation of Hazardous Encounter Events for Merchant and Fishing Vessels: The paper introduces a method to assess encounter risk data for merchant and fishing vessels. By calculating the CPA and TCPA, the collision risk is quantified. The experiment sets the vessel domain for fishing vessels engaged in operations to 0.5 nautical miles, ensuring a safe distance of at least 0.5 nautical miles between each vessel in a collaborative operation. The paper categorizes and assesses risk data for different encounter situations.

3. Visualization of High-Risk Collision Areas for Merchant and Fishing Vessels: The paper conducts a visual analysis of high-risk collision areas for merchant and fishing vessels in the research area under different encounter situations. The identified high-risk collision areas include the eastern nearshore waters of Lianjiang, with latitude ranging from 26°17'56.40" to 26°25'12", with longitude between 119°24'25.20" and 119°48'7.20" and the Minjiang River Estuary. The paper validates the identified high-risk collision areas using data on the locations of maritime collisions in the research area over the past three years, demonstrating the reasonableness of the experiment's outcomes.

In conclusion, ship collision accidents result from a combination of various factors. To more accurately assess collision risk, future efforts could involve fusing data collected by multiple sensors, such as video and radar data. Comprehensive considerations, including visibility and navigation

density, should be incorporated to judge collision risk during encounters. In this study, the occurrence of a vessel intruding into the safety navigation domain is considered as indicating collision risk. However, it is crucial to note that the presence of collision risk does not guarantee an actual collision. In future study, building upon this premise, emerging technologies such as deep learning can be leveraged to construct vessel trajectory prediction models. These models can be used to estimate the time and location of potential collisions in scenarios where collision avoidance maneuvers are not implemented.

References

1. Sedov, V.A.; Sedova, N.A.; Glushkov, S.V. The fuzzy model of ships collision risk rating in a heavy traffic zone. *Vibroengineering Procedia* **2016**,8,453-458.
2. Yi, M. Design of the model for predicting ship collision risk using fuzzy and DEVS. Journal of the Korea Society for Simulation **2016** 25,127-135.
3. Chin, H.C.; Debnath, A.K. Modeling perceived collision risk in port water navigation. Safety Science **2009**,47,1410-1416.
4. Liu, K.; Yu, Q.; Yuan, Z.; Yang, Z.; Shu, Y. A systematic analysis for maritime accidents causation in Chinese coastal waters using machine learning approaches. *Ocean & Coastal Management* **2021**, 213, 105859
5. Yu, Y.; Chen, L.; Shu, Y.; Zhu, W. Evaluation model and management strategy for reducing pollution caused by ship collision in coastal waters. *Ocean & Coastal Management* **2021**, 203, 105446.
6. Shinoda, T.; Shimogawa, K.; Tamura, Y. Applied Bayesian Network Risk Assessment for Collision Accidents between Fishing

   Vessels and Cargo Vessels. *Journal of Institute Navigation* **2012**, 127, 165-174.
7. Takemoto, T.; Sakamoto, Y.; Yano, Y.; Furusho, M. Collision Avoidance Actions and Backgrounds in Fishing Vessels Collision

   Accidents. *The Journal of Japan Institute of Navigation* **2010**, 122, 113-120.
8. Xiao, F.; Ma, Y.; Wu, B. Review of Probabilistic Risk Assessment Models for Ship Collisions with Structures. *Applied Sciences* **2022**. 12, 3441.
9. Mou, J.M.; Van der Tak, C.; Ligteringen, H. Study on collision avoidance in busy waterways by using AIS data. *Ocean Engineering* **2010**. 37,483-490.
10. Uğurlu, F., Yıldız, S., Boran, M., Uğurlu, Ö., & Wang, J. Analysis of fishing vessel accidents with Bayesian network and Chi-square methods. *Ocean Engineering*, **2020**. 198, 106956.
11. Argüelles, R. P., Maza, J. A. G., Martín, F. M., & Bartolomé, M. Ship-to-ship dialogues and agreements for collision risk reduction. *The Journal of Navigation*, **2021**. 74(5), 1039-1056.
12. Huang, Y.; Chen, L.; Negenborn, R.R.; Van Gelder, P. A ship collision avoidance system for human-machine cooperation during

    collision avoidance. *Ocean Engineering* **2020**, 217, 107913.
13. Jung, C.H. A study on the requirement to the fishing vessel for reducing the collision accidents. *Journal of the Korean society of marine environment & safety* **2014**, 20, 18-25.
14. Yang, J.; Sun, Y.; Song, Q.; Ma, L. Laws and preventive methods of collision accidents between merchant and fishing vessels in

coastal area of China. *Ocean & Coastal Management* **2023**, 231, 106404.

15. Wang, X.; Zhou, Z.; Liu, Y.; Song, H. Discussions about the best methods of collision between merchant ships and fishing boats

during fishing seasons near Chinese coast. In Proceedings of the International Conference on Computer Information Systems and Industrial Applications. *Atlantis Press* **2015**, pp. 758-761.

16. Obeng, F.; Domeh, V.; Khan, F.; Bose, N.; Sanli, E. Capsizing accident scenario model for small fishing trawler. *Safety science* **2022**, 145, 105500.

17. Chou, C.c. Application of ANP to the selection of shipping registry: The case of Taiwanese maritime industry. *International*

Journal of Industrial Ergonomics **2018**, 67, 89-97.

18. Seo, A.; Hida, T.; Nishiyama, M.; Nagao, K. Comparison and evaluation on user interface of small ship navigation support

system. *Proceedings of the Japan Institute of Navigation* **2018**, pp. 1-4.

19. Ma, F.; Chu, X.; Yan, X.; Liu, C. ERROR DISTINGUISH OF AIS BASED ON EVIDENCE COMBINATION. *Journal of Theoretical & Applied Information Technology* **2012**,45,83-90.

20. Ma, F.; Chu, X.; Liu, C. The error distinguishing of automatic identification system based on improved evidence similarity. In

ICTIS 2013: Improving Multimodal Transportation Systems-Information, Safety, and Integration; **2013**; pp. 715-722.

21. Fujii, Y.; Tanaka, K. Traffic capacity. *The Journal of navigation* **1971**, 24, 543-552.

22. Kearon, J. Computer Programs for Collision Avoidance and Traffic Keeping. In Proceedings of the Conference on Mathematical

Aspects on Marine Traffic, London,**1997**.

23. Li, H.; Weng, J; Zhou, Y. Ship collision avoidance method in starboard-to-starboard head-on situations. In Proceedings of the

2023 7th International Conference on Transportation Information and Safety (ICTIS). IEEE, **2023**, pp. 609-614.